Eur. Phys. J. B **55**, 355–362 (2007)
DOI: 10.1140/epjb/e2007-00072-0

THE EUROPEAN PHYSICAL JOURNAL B

The two-dimensional Peierls-Nabarro model for interfacial misfit dislocation networks of cubic lattice

Y. Zhang[1] and Y. Yao[2,a]

[1] Department of Physics, Beijing Normal University, Beijing 100875, P.R. China
[2] Beijing National Laboratory for Condensed Matter Physics, Institute of Physics, Chinese Academy of Sciences, Beijing 100080, P.R. China

Received 4 August 2006 / Received in final form 15 January 2007
Published online 14 March 2007 –

Abstract. A model is developed to investigate the two-dimensional interfacial misfit dislocation networks that follows the original Peierls-Nabarro idea. Structure and energies of heterophase interfaces are considered for the cubic lattice. To examine the energy contribution of misfit dislocations, where interactions between two dislocation arrays are concerned, a generalized stacking fault energy is proposed. Combined with first-principles calculations, we apply this model to a practical metal-ceramic example: the Ag/MgO(100) interface. An important correction to the adhesive energy is proposed in addition to its dislocation structure being confirmed.

PACS. 68.35.-p Solid surfaces and solid-solid interfaces: Structure and energetics – 61.72.Bb Theories and models of crystal defects – 61.72.Lk Linear defects: dislocations, disclinations

1 Introduction

The interfaces between dissimilar materials are prevalent in numerous industrial applications, such as heterostructure devices, metal-ceramic composites, and protective coatings [1], which has resulted in the topic receiving much attention over the past two decades. It is of vital importance to understand their atomic structure and adhesive energy since they control the properties and performance of materials. In almost all of these interfaces, misfit dislocations (MD) are geometrically necessary defects, naturally forming part of the interfacial structure.

To determine atomic structures and energies of MDs at heterophase interfaces is complicated. Firstly, they are difficult to be determined experimentally [2–4]. The best theoretical tools for solving this problem are expected to be those based on first-principles calculations. Some studies have been made [5,6]; however, reliable results have been reported only for a few cases with rather short periodic structures. Normally, in the case of long periodic structures such as for MDs, the required system size will be beyond presently available computational capacity. Consequently, interfacial MDs have been neglected. Instead, the coherent interface approximation (CIA) is used to deal with interfaces that possess long periodic dislocation structures, such as metal-ceramic interfaces. However, estimates for theoretical adhesive energies calculated using the CIA, being much larger than observed values, are controversial [5].

[a] e-mail: ygyao@aphy.iphy.ac.cn

An alternative theoretical framework is the Peierls-Nabarro (PN) model [7,8], which employs multiscale techniques. It can provide quantitative estimates of atomic property of MDs. The generalized one-dimensional (1D) PN model for an interfacial MD array had been proposed by Yao et al. [9], in which a concise expression for the displacement field of the MD had been derived. Recently, this formalism has been successfully applied in a study of the NiAl/Mo interface [10], and the Fe(100)/VN(100) interface [11].

In previous studies based on PN models, it is always assumed that the misfit occurs only in one single direction, or in two independent directions without any interaction. Hence, one obtains either an approximate solution [8], or a more precise solution [9], by dealing with the 1D interfacial MD array. In fact, for real interfaces, lattice misfit usually occurs in two dimensions. Thus, in general cases, a 1D MD model will provide an inadequate description the two-dimensional (2D), periodic, interactive dislocation network structure which appears at the interface. A generalized two-dimensional PN model will be developed in this work, and will be applied to model heterophase interfaces possessing 2D dislocation networks.

Without loss of generality, following reference [9], we consider a bilayer composed from two cubic crystals, 1 (upper), and 2 (lower), joined at (001) surfaces, with a MD network (the dislocation core) positioned at the interface. The Ox_3 axis is chosen to be directed toward the upper crystal, and is perpendicular to the plane of the interface Ox_1x_2. The MD network is always aligned along

the crystallographic directions $\langle \boldsymbol{b} \rangle$ with Burgers vector $\boldsymbol{b}_i$, and character $\langle \boldsymbol{l} \rangle$ where the line directions are $\boldsymbol{l}_i$ $(i = 1, 2)$, similar to the definition in reference [2]. In the following, we will denote a MD network by $\{\langle \boldsymbol{b} \rangle; \langle \boldsymbol{l} \rangle\}$. For the system concerned, we adopt the conventional assumptions: (i) the crystals 1 and 2 have lattice parameters a_1 and a_2, respectively $(a_1 > a_2)$; (ii) a_1 and a_2 may be generated from a reference lattice with parameter c defined by[8] as follows.

$$p = Pa_1 = (P+1)\, a_2 = \left(P + \frac{1}{2}\right) c, \tag{1}$$

where P is an integer; and (iii) the crystals behave as isotropic elastic media in their response to applied forces, with shear moduli μ_1, μ_2, and Poisson's ratios ν_1, ν_2, respectively. Equation (1) defines the MD spacing p, parameter c, and misfit f as

$$\begin{aligned} p &= \frac{a_1 a_2}{a_1 - a_2}, \\ c &= \frac{2a_1 a_2}{(a_1 + a_2)}, \\ f &= \frac{c}{p} = \frac{2\,(a_1 - a_2)}{(a_1 + a_2)}. \end{aligned} \tag{2}$$

A multiscale method is employed here to investigate the interface, and a suitable energy function is developed to describe the interface system. The two sides of the interface are treated by the elastic continuum theory, while the interface is treated by atomic theory. Similar to the original PN model, the energy of the MD is calculated as the sum of two contributions: the elastic strain energy stored in the two semi-infinite elastic media of E_{elastic1}, and E_{elastic2}, and the misfit energy associated with the distortion of atomic bonds across the interface [12], E_{misfit}. Thus, the total energy of the system can be expressed by

$$E_{\text{tot}} = E_{\text{elastic1}} + E_{\text{elastic2}} + E_{\text{misfit}}. \tag{3}$$

In the following sections, we will derive the three parts of the total energy as functions of the elastic displacement field of the interface, then solve the minimum energy problem to find the interfacial structure and energy. In the final section, we will apply the method to a model Ag/Mg(100) interface, and discuss the results for its atomic structure and adhesive energy.

2 Calculation of elastic energies

When two semi-infinite crystals adhere to one another to form an interface, the atoms at the interface bond together so that the atoms on each side are displaced from their normal lattice sites, and relax to a new equilibrium structure that is described by a unique displacement field around the interface. Modern atomic simulations find that most interfaces have periodic structures. This section deals with how the elastic energy is distributed in two semi-infinite media for a given interfacial displacement field.

Let the displacement field of the upper half plane be $\boldsymbol{u}^+(x_1, x_2, 0)$, while the lower one be $\boldsymbol{u}^-(x_1, x_2, 0)$. The normal force in the interface is given as $p_{33}(x_1, x_2, 0) = 0$. Based on the results reported in reference [8], we can estimate that the relative error of the total energy due to this assumption is about 10%. Therefore, this is an elastic problem about two semi-infinite bulk media given the corresponding displacement field $\boldsymbol{u}^+(x_1, x_2, 0)$, $\boldsymbol{u}^-(x_1, x_2, 0)$, and the resulting normal force $p_{33}(x_1, x_2, 0) = 0$.

Let us now apply the following treatment to the system. For the upper semi-infinite material 1, we move some material 1 to its lower semi-infinite part, and make the interfacial displacement field of the replenishing material opposite to the upper part; i.e. $-\boldsymbol{u}^+(x_1, x_2, 0)$. Hence, we create isotropic medium (I) containing a planar dislocation network. For the lower infinite material 2, we apply the equivalent procedure as done for 1, now using $-\boldsymbol{u}^-(x_1, x_2, 0)$ for the corresponding interfacial displacement field. This creates isotropic medium (II) with its own planar dislocation network. Hence, the elastic energy of our original two semi-infinite media now becomes half of the total elastic energy of these two infinite, bulk, isotropic media with planar dislocation networks: i.e. half of medium (I)'s contribution added to half of medium (II)'s.

For the case of an infinite, periodic, planar dislocation network in an infinite, isotropic, elastic medium, we will apply Kröner and Rey's [13] formalism to construct the elastic energy solution. Let $\boldsymbol{r}$ be a vector with coordinates (x_1, x_2, x_3), $\boldsymbol{\rho}$ any vector in the plane Ox_1x_2, and $\boldsymbol{n}$ the unit normal vector of the interface plane. Then, the plane dislocation density tensor $\boldsymbol{\alpha}^*(\boldsymbol{\rho})$ has a distribution in one cell that can be written as

$$\boldsymbol{\alpha}^{*(\boldsymbol{n})}(\boldsymbol{\rho}) = \boldsymbol{n} \times \boldsymbol{\beta}^P. \tag{4}$$

Here, $\boldsymbol{\beta}^P_{ij} = \partial u^P_j / \partial x_i$ is the strain in one cell, and u^P_j is the plastic displacement field, which is $2u^+_j$ in medium (I), and is $2u^-_j$ in medium (II), respectively.

Following Kröner and Rey [13] the incompatibility tensor $\boldsymbol{\eta}$ is defined as

$$\eta_{il} = \text{Sym}(\varepsilon_{ijk}\alpha_{lj,k}). \tag{5}$$

Here, Sym( ) means that we take only the symmetrical part of the tensor inside the brackets, ε_{ijk} is the permutation tensor, and $\alpha_{lj,k}$ holds for $\partial\alpha_{lj}/\partial x_k$.

The self-energy per unit surface for a periodic planar distribution of a MD network can then be calculated using

$$E_{\text{elastic}} = \frac{1}{2s_0} \int_{S_0} \eta_{ij}(x_1, x_2, x_3)\chi_{ij}(x_1, x_2, x_3) dx_1 dx_2 dx_3. \tag{6}$$

Here, $\chi_{ij} = 2\mu(\chi'_{ij} + [\nu/(1-\nu)]\chi'_{kk}\delta_{ij})$, μ and ν are the shear moduli and Poisson ratio, respectively. s_0 is the area per unit cell, and χ' can be obtained from $\nabla^4\chi' = \eta$ [13].

For medium (I), we label the corresponding quantities α^*, η, χ, and χ' with a superscript '+'. By the process set out above, the elastic energy of the original semi-infinite material 1 can be determined. In medium (II), we

label quantities with a superscript '−'. The elastic energy of the original semi-infinite material 2 can be obtained in a similar manner. Then, the elastic energy of the semi-infinite material 1 and the semi-infinite material 2 are described by

$$E_{\text{elastic1}} = \frac{1}{4s_0}\int\limits_{S_0} \eta_{ij}^{+}(x_1,x_2,x_3)\chi_{ij}^{+}(x_1,x_2,x_3)dx_1dx_2dx_3, \tag{7}$$

and

$$E_{\text{elastic2}} = \frac{1}{4s_0}\int\limits_{S_0} \eta_{ij}^{-}(x_1,x_2,x_3)\chi_{ij}^{-}(x_1,x_2,x_3)dx_1dx_2dx_3, \tag{8}$$

respectively.

3 Misfit energy

The atomic misfit energy E_{misfit} in the glide interface plane can be determined by the generalized stacking fault energy γ-surface [14] (energy per unit area), which describes the atomic misfit energy when the two semi-infinite crystals are shifted rigidly against each other by a vector $\boldsymbol{U}$. Accurate γ-surfaces are usually generated from first-principles calculations. Here, we represent the generalized stacking fault energy γ-surface by a two-dimensional Fourier series, following the idea of reference [15]. We assume: (i) the crystals possess cubic symmetry; (ii) the misfit dislocations of the interface is described according to a reference lattice with parameter c. The simplest expression for the generalized γ-function can take the form

$$\begin{aligned}\gamma\left(U_1,U_2\right) = \frac{\tau_0 c}{4\pi^2}\Bigg[\,&\zeta\left(2-\cos\frac{2\pi U_1}{c}-\cos\frac{2\pi U_2}{c}\right)\\ &+\left(\frac{1-\zeta}{2}\right)\left(2-\cos\frac{2\pi\left(U_1+U_2\right)}{c}\right.\\ &\left.-\cos\frac{2\pi\left(U_1-U_2\right)}{c}\right)\Bigg].\end{aligned} \tag{9}$$

Here, c is defined in equation (2), τ_0 and ζ are adjustable coefficients. τ_0 represents the bond strength parallel to the interface, and ζ represents the shape of the γ-surface. $\boldsymbol{U} = (U_1, U_2, 0)$ is the relative displacement between corresponding atoms on each side, which is the combined plastic displacement and misfit displacement. The atomic misfit displacement is the intrinsic relative displacement that, due to the unequal lattice parameter $a_1 \neq a_2$, is induced when crystal 1 and crystal 2 join each other to form the interface, under the condition of no distortion occurring.

Thus, $\boldsymbol{U} = (U_1, U_2, 0)$ can be expressed by $\boldsymbol{u}(x_1, x_2, 0)$[8]:

$$\begin{aligned}U_1\left(x_1,x_2\right) &= \frac{c}{2}+\frac{c}{p}x_1+u_1^{+}\left(x_1,x_2,0\right)-u_1^{-}\left(x_1,x_2,0\right)\\ U_2\left(x_1,x_2\right) &= \frac{c}{2}+\frac{c}{p}x_2+u_2^{+}\left(x_1,x_2,0\right)-u_2^{-}\left(x_1,x_2,0\right)\end{aligned} \tag{10}$$

where $c/2 + c/px_1$ and $c/2 + c/px_2$ represent the atomic misfit displacement contribution along the two orthogonal axes, respectively.

The γ-function in equation (9) yields a variety of γ-surfaces: see Figure 1. Notice that it changes strongly with the adjustable coefficient ζ. The larger that ζ is, the higher the peak at the centre of the γ-surface rises, $\gamma(c/2, c/2)$. The generalized stacking fault energy γ-surface expressed in this form has two merits: (i) when $U_1 = 0$, or $U_2 = 0$, it reduces to a simple cosine function which is dependent on τ_0 only; (ii) when $\zeta = 1$, $\gamma(U_1, U_2) = \frac{\tau_0 c}{4\pi^2}(2 - \cos\frac{2\pi U_1}{c} - \cos\frac{2\pi U_2}{c})$, and the 2D dislocation network problem degenerates into the 1D dislocation array problem, which can be solved by the method in reference [8] or [9].

Given the generalized stacking fault energy γ-surface, the average interface misfit energy is then

$$E_{\text{misfit}} = \frac{1}{s_0}\int\limits_{S_0}\gamma\left(U_1\left(x_1,x_2\right),U_2\left(x_1,x_2\right)\right)dx_1dx_2. \tag{11}$$

4 Total interface energy

Combining the results above, the total interface energy per unit area for the periodic interface system is

$$\begin{aligned}E_{\text{tot}} = &\frac{1}{4s_0}\int\limits_{S_0}\eta_{ij}^{+}(x_1,x_2,x_3)\chi_{ij}^{+}(x_1,x_2,x_3)dx_1dx_2dx_3\\ &+\frac{1}{4s_0}\int\limits_{S_0}\eta_{ij}^{-}(x_1,x_2,x_3)\chi_{ij}^{-}(x_1,x_2,x_3)dx_1dx_2dx_3\\ &+\frac{1}{s_0}\int\limits_{S_0}\gamma\left(U_1\left(x_1,x_2\right),U_2\left(x_1,x_2\right)\right)dx_1dx_2.\end{aligned} \tag{12}$$

Naturally, the equilibrium elastic displacement field $\boldsymbol{u}^{+}$ and $\boldsymbol{u}^{-}$ must lead to an global minimum for E_{tot}. In order to minimize the energy function E_{tot} numerically, the usual approach is to discretize space. The continuous space is thereby uniformly divided into many small regions, where each of the regions is represented by one discrete point. The displacement of the discrete points position, therefore, becomes a variable in the energy minimization procedure.

The plastic strain, for the elastic energies mentioned above, is treated by a similar discrete scheme: $\boldsymbol{\beta}_{ij}^{P} = [u_j(I, J+1) - u_j(I, J)]/\Delta x_i$, where I, J indicate the

position coordinate of the corresponding discrete space. Then, the plane dislocation density tensor $\boldsymbol{\alpha}$ can be derived from equation (4). Finally, the incompatibility tensor $\boldsymbol{\eta}$ is treated similarly. Once the incompatibility tensor $\boldsymbol{\eta}$ is known, the strain energy can be obtained from equation (6). In this process, the critical problem is how to obtain χ and χ'. Here, we follow Rey and Saada's work [13], the details of which are shown in the Appendix.

The total energy of the interface system, finally, can be expressed in terms of the variables $u_1^+(I,J)$, $u_1^-(I,J)$, $u_2^+(I,J)$, and $u_2^-(I,J)$; i.e., $E_{\rm tot} = E_{\rm tot}(u_1^+(I,J), u_2^+(I,J), u_1^-(I,J), u_2^-(I,J))$. By minimizing the total energy, we can obtain the displacement field $u_1^+(I,J)$, $u_1^-(I,J)$, $u_2^+(I,J)$, and $u_2^-(I,J)$. Furthermore, the energies of the interface, the stress field, and the strain field can also be determined.

In the computation, we adopt Newton's method to minimize the energy. For the special case of $\zeta = 1$, $\gamma(U_1,U_2) = \frac{\tau_0 c}{4\pi^2}(2 - \cos\frac{2\pi U_1}{c} - \cos\frac{2\pi U_2}{c})$, and there is no interaction between the two MD arrays with different directions. The 2D MD network degenerates into two independent 1D arrays, for which an analytical solution exists [9]. Our computational result is in agreement with this analytical solution.

5 The interaction between two MD arrays with orthogonal directions

In general, according to the classic elasticity theory of Volterra dislocations, interaction occurs between a pair of MD arrays with different directions. Hence, the interfacial energy of a periodic MD network is usually not equal to the net energy of two 1D dislocation arrays. We know that only in the special case with $\zeta = 1$, can $\gamma(U_1,U_2)$ be decomposed into $f(U_1)+f(U_2)$, meaning that the two parts have no interaction; otherwise, one must consider the contribution of their interaction to the total interface energy.

Figure 2 illustrates the relationship between the total interface energy and ζ with different values of τ_0 and misfit parameter $f(= c/p)$. Since the total interface energy corresponds to the special case of no interaction between the two intersecting dislocation arrays, we can study their interaction by how much the total interface energy differs from $E_{\rm tot}(\zeta = 1)$. When τ_0 is large and the misfit parameter f is small; over a range of ζ, the interface energy remains close to $E_{\rm tot}(\zeta = 1)$ (see Fig. 2). From this behaviour, we can conclude that the interaction is weak. The range for nearly no interaction is $\zeta > 0.1$, when $\tau_0 = 10\mu$ and $f = 0.1$; and the range is $\zeta > 0.5$, for $\tau_0 = 3\mu$ and $f = 0.1$. However, interaction between the two dislocation arrays cannot be neglected when τ_0 is small and f is large, such as $\tau_0 = 0.1\mu$ and $f = 0.1$ (see Fig. 2). The more τ_0 decreases and f increases, the larger the ratio of the dislocation core is in comparison with to the global interface area. Figure 3 illustrates the effect of τ_0 on the interface displacement field. The misfit parameter f produces similar behaviour.

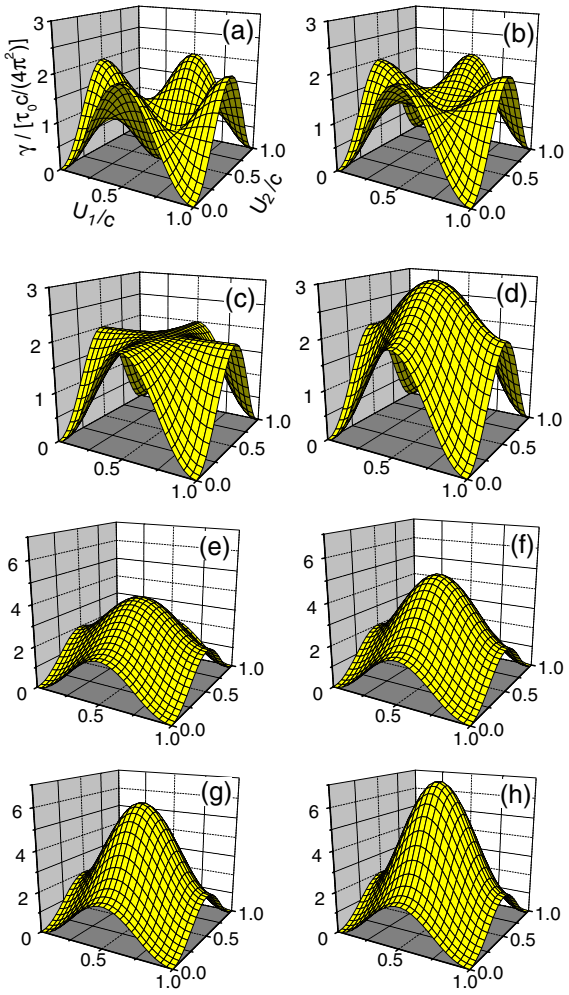

Fig. 1. The generalized stacking fault energy γ-surface. (a) $\zeta = 0$; (b) $\zeta = 0.25$; (c) $\zeta = 0.5$; (d) $\zeta = 0.75$; (e) $\zeta = 1$; (f) $\zeta = 1.25$; (g) $\zeta = 1.5$; (h) $\zeta = 1.75$. The labels indicated in (a) apply to all.

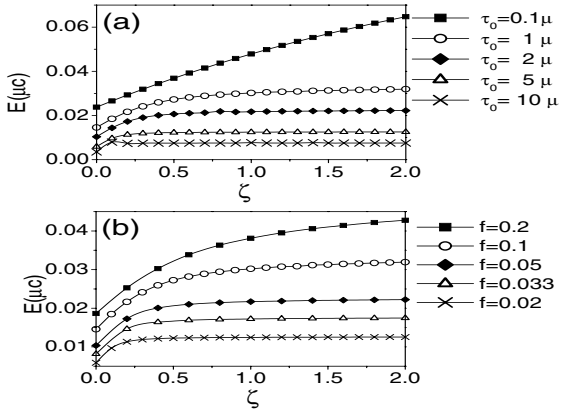

Fig. 2. The total interface energy versus ζ. (a) τ_0 is set at five different values as indicated in the diagram, while all other parameters are held fixed: $c = 1$, $f = 0.1$, $\mu_1 = \mu_2 = \mu$, $\nu = 0.3$; (b) f is set at five different values as indicated in the diagram, while all the other parameters are held fixed: $c = 1$, $\tau_0 = \mu_1 = \mu_2 = \mu$, and $\nu = 0.3$.

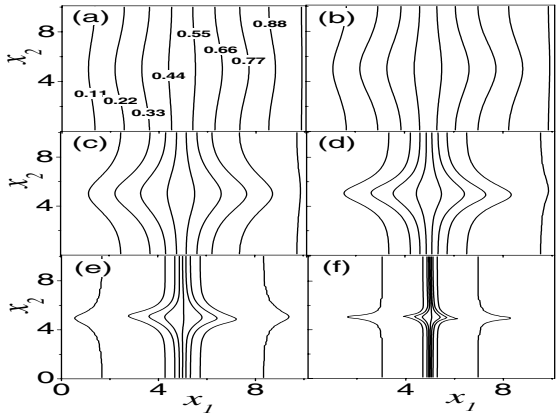

Fig. 3. The dislocation structure corresponding to different τ_0 values, i.e., isolines of the interface displacement field U_1. (a) $\tau_0 = 0.1\mu$; (b) $\tau_0 = 0.2\mu$; (c) $\tau_0 = 0.5\mu$; (d) $\tau_0 = 1\mu$; (e) $\tau_0 = 2\mu$; (f) $\tau_0 = 5\mu$. All the other parameters are held fixed: $c = 1$, $f = 0.1$, $\mu_1 = \mu_2 = \mu$, $\nu = 0.3$, and $\zeta = 0.5$.

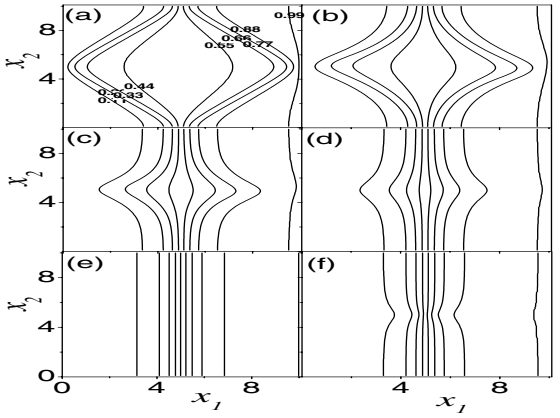

Fig. 4. The dislocation structure corresponding to different γ-surfaces, i.e., isolines of the interface displacement field U_1. (a) $\zeta = 0$; (b) $\zeta = 0.25$; (c) $\zeta = 0.5$; (d) $\zeta = 0.75$; (e) $\zeta = 1$; (f) $\zeta = 1.25$. All the other parameters are held fixed: $c = 1$, $f = 0.1$, $\tau_0 = \mu_1 = \mu_2 = \mu$, and $\nu = 0.3$.

We know that interaction between the two dislocation arrays is related to the generalized γ-surface (ζ), and the effect of γ-surface mostly depends on the structure of dislocation core (see Figs. 1–3). Thus, if the dislocation core is relatively small, then the interaction contributes little to the total interface energy. Only in these circumstances can the 1D PN model describe the interface system adequately [9].

The dislocation line expands when $\zeta > 1$, and shrinks when $\zeta < 1$ (see Fig. 4). For a given τ_0 and f, the larger $|\zeta - 1|$ is, the greater is the distortion the displacement field in dislocation core, and structure of the interface MD network responds accordingly. For example, the MD network appears as $N_1 = \{\frac{1}{2}\langle 110\rangle; \langle 110\rangle\}$ when $\zeta = 0$ (see (a) in Fig. 4), in contrast with $N_2 = \{\frac{1}{2}\langle 100\rangle; \langle 100\rangle\}$ when $\zeta = 1$ (see (e) in Fig. 4).

6 Application to the Ag/MgO(100) interface

The Ag/MgO(100) interface has been studied extensively. Recent experiments have come to two different conclusions. In one study based on high resolution transmission electron microscopy (HRTEM) observations [2], the structure proposed for the dislocation networks is $N_2 = \{\frac{1}{2}\langle 100\rangle; \langle 100\rangle\}$. The other study concludes from grazing incidence x-ray scattering (GIXS) measurements [3] that it is $N_1 = \{\frac{1}{2}\langle 110\rangle; \langle 110\rangle\}$. We aim to resolve this by applying our model to the Ag/MgO(100) interface.

Based purely on geometric arguments, the coincidence-site lattice (CSL) theory [16] is used to construct the initial atomic positions of the Ag/MgO(100) interface. Previous first-principles calculations predict that the silver atoms at the interface prefer to lie above oxygen ions on the substrate instead of magnesium ions, when both the Ag and MgO crystals are cut and joined along their $\langle 001\rangle$ directions. Consequently, this suggests that the coincidence-site points are as follows. The positions of the O atoms of the unrelaxed MgO lattice are located exactly above above all the unrelaxed Ag atoms, so that a square CSL oriented along $\langle 110\rangle$ directions is obtained. The CSL lattice possesses 95.6 Å periodicity in one cell, of which the period of the MgO ceramic is 32 and Ag metal is 33.

In order to apply our model, it is important to construct an appropriate generalized stacking fault energy γ-surface for the Ag/MgO(100) interface. This is done by fitting the γ-function to results from first-principles calculations. These are taken from the work of Schönberger et al. who used the linear muffin-tin orbital (LMTO) method in their study of the Ag/MgO(100) interface [17]. In their model, the metal was stretched uniformly parallel to the interface to match the ceramic substrate in three different translation states: a Ag atom above a hole, a Ag atom above a Mg atom, and a Ag atom above an O atom. The adhesive energies corresponding to the three translation states are: 0.6 eV, 0.4 eV, and 0.8 eV, respectively. Using these three values in the γ-function (9) yields $\tau_0 = 34.1$ GPa and $\zeta = 0.856$. The elastic parameters used in our calculation are, $\mu_{\mathrm{Ag}} = 33.8$ GPa, $\nu_{\mathrm{Ag}} = 0.354$; $\mu_{\mathrm{MgO}} = 129$ GPa, and $\nu_{\mathrm{MgO}} = 0.173$ [12].

Figure 5 shows the relative displacement field of the interfacial atoms U_1 and U_2, which are defined in equation (10). The MD network in Figure 5 is $N_1 = \{\frac{1}{2}\langle 110\rangle; \langle 110\rangle\}$ type with pure edge character: i.e. it is oriented along $\langle 110\rangle$ directions with $\frac{1}{2}\langle 110\rangle$ Burgers vectors. This is in agreement with Renaud et al.'s observations [3], and different from Trampert et al.'s study[2]. The conclusion from the HRTEM[2] experiments appears doubtful, because the $\{110\}$ cross-section was not observed, and the image of the $\{100\}$ cross-section reported is unclear.

The positions of the interfacial atoms are shown in Figure 6, from which it can be seen clearly that the MD network is $N_1 = \{\frac{1}{2}\langle 110\rangle; \langle 110\rangle\}$ type. Due to the interaction between the two perpendicular arrays, the dislocation lines expand outwards slightly in the core of overlapping sub-lattices, as illustrated in Figure 5. Clearly, their interaction is weak. From Figure 5, we can also estimate that

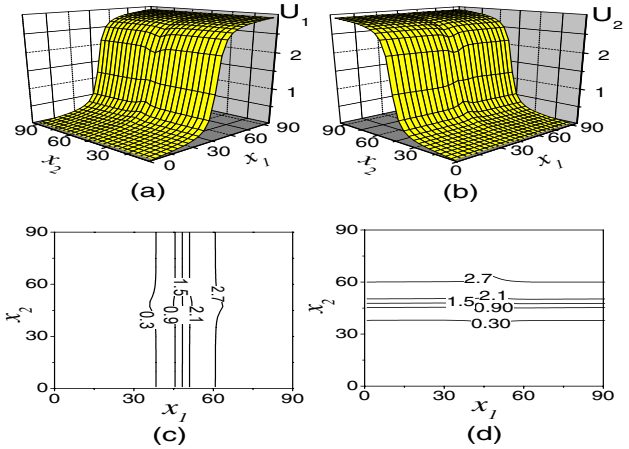

Fig. 5. The relative displacement field of the Ag/MgO(100) interfacial atoms. (a) $U_1(x_1, x_2)$; (b) $U_2(x_1, x_2)$; (c) and (d) are the isoline graph of (a) and (b). The units of both U_1 and U_2 are Å. The axes x_1 and x_2 are along the ⟨110⟩ crystallographic directions, respectively.

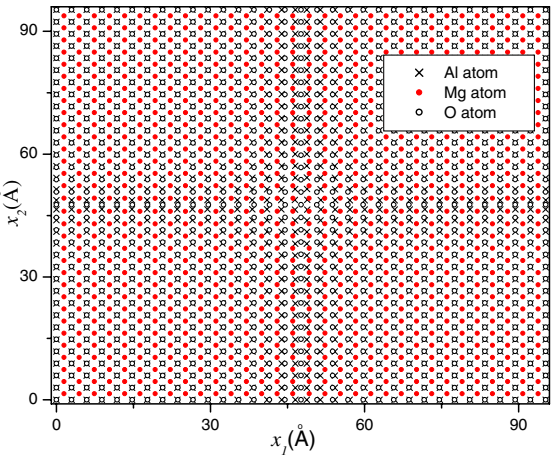

Fig. 6. Schematic map of the Ag/MgO(100) interface. The axes x_1 and x_2 are along the ⟨110⟩ crystallographic directions, respectively.

the half-width of the MD is about 6.6 Å, i.e. approximately 2.3 times the interatomic distance.

Figure 7 plots the elastic displacement field of the Ag/MgO(100) interface system. From this, it is estimated that the elastic strain in the Ag at the interface is about three times of that in the MgO, i.e. approximately the ratio $[\mu_{\mathrm{MgO}}/(1-\nu_{\mathrm{MgO}})]$:$[\mu_{\mathrm{Ag}}/(1-\nu_{\mathrm{Ag}})]$. The largest elastic displacements are about 0.65 Å and 0.22 Å for Ag metal and MgO ceramic, respectively.

We also calculate the interfacial energies: the misfit energy is 0.100 $\mathrm{J\,m^{-2}}$, the elastic energy stored in the Ag is 0.085 $\mathrm{J\,m^{-2}}$, the elastic energy stored in the MgO is 0.0285 $\mathrm{J\,m^{-2}}$, making the total elastic energy 0.114 $\mathrm{J\,m^{-2}}$, and the total interface energy in the system 0.214 $\mathrm{J\,m^{-2}}$. This is significantly smaller than the total interface energy 0.313 $\mathrm{J\,m^{-2}}$ calculated previously using our 1D PN model[9]. In addition to the interaction among

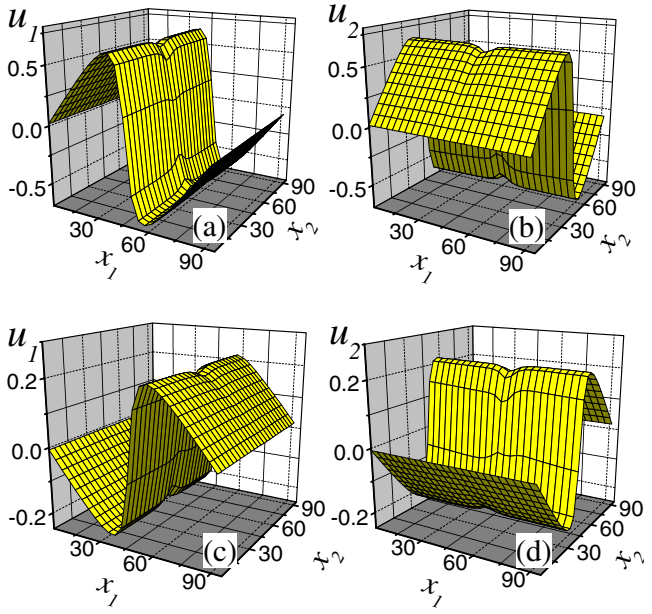

Fig. 7. The elastic displacement field $u_1(x_1, x_2)$ and $u_2(x_1, x_2)$ of the Ag/MgO(100) interface. (a) and (b) are the field in the Ag metal; while (c) and (d) are the field in the MgO ceramic. The units of both u_1 and u_2 are Å. The axis x_1 and x_2 are along the ⟨110⟩ crystallographic directions, respectively.

dislocations in the 2D model, the difference between the two values is mainly due to the MD network being N_1 type in the present work, while being assumed to be N_2 type in Ref. [9]. Crucially, the 2D PN model, can automatically predict the dislocation network type, while in 1D PN model cannot.

Finnis [5] pointed out that when the interfacial MD network is neglected, the adhesive energy resulting from first-principles calculations using the CIA will be larger than the experimental value (0.45 ± 0.1) $\mathrm{J\,m^{-2}}$. Thus, the true adhesive energy is smaller by an amount equal to the total interface energy considered in this work. Among several theoretical estimates, the one closest to the measured value is 0.9 $\mathrm{J\,m^{-2}}$ [6]. Subtracting the total interface energy calculated in this work from it leaves approximately 0.7 $\mathrm{J\,m^{-2}}$. Although this is still larger than the measured energy, the discrepancy has been reduced. In our opinion, future prospects for improving agreement between theory and experiment are good.

7 Summary and conclusion

A model that follows the original Peierls-Nabarro idea is proposed to treat 2D interfacial MD networks. Atomic structures and energies are considered, and the generalized stacking fault energy γ-surface is explored in detail. The interaction between the two orthogonal dislocation arrays at the interface between two dissimilar cubic crystals is discussed. The method is applied to a model Ag/MgO(100) interface, representing a practical example. Its dislocation network type is confirmed as

being $N_1 = \{\frac{1}{2}\langle 110\rangle; \langle 110\rangle\}$. First-principles calculations on their own overestimate the adhesive energy. This discrepancy is reduced significantly by including the total interface energy calculated here. Thus, our formalism represents an important correction, which originates from the elastic and the misfit energies of the system. Although the systems considered here are (001) faces of cubic lattices only, this method can, in principle, be directly extended without any difficulty to other types of lattice. We expect this multiscale method may be applied in understanding other complicated interface systems.

This work was supported by the Knowledge Innovation Project of the Chinese Academy of Sciences (NSFC) grant Nos. 10404035, 10534030, 10674163.

Appendix

In this appendix, we apply Kröner's theory to calculate the elastic energy for the case of a 2D periodic, planar dislocation network, and provide the full expressions for the tensors, $\boldsymbol{\eta}$, $\boldsymbol{\chi}$, and $\boldsymbol{\chi'}$, etc.

Assuming that the 2D periodic translation lattice vectors are $(\boldsymbol{a^{(1)}}, \boldsymbol{a^{(2)}})$, we can define reciprocal lattices $(\boldsymbol{g^{(1)}}, \boldsymbol{g^{(2)}})$ by $\boldsymbol{g^{(i)} \cdot a^{(j)} = \delta_{i,j}}$. Hence, the planar dislocation density tensor $\boldsymbol{\alpha}$ can be expressed in a Fourier series:

$$\boldsymbol{\alpha}^* (\boldsymbol{\rho}) = \sum_{g} \boldsymbol{\alpha}^{*(\boldsymbol{g})} \exp 2\pi i \boldsymbol{g\rho}, \tag{13}$$

in which

$$\boldsymbol{\alpha}^{*(\boldsymbol{g})} (\boldsymbol{\rho}) = \frac{1}{s_0} \int\limits_{S_0} \boldsymbol{\alpha}^* (\boldsymbol{\rho}) \exp (-2\pi i \boldsymbol{g\rho})\, dx_1 dx_2. \tag{14}$$

Here, s_0 is the area of a unit cell. From equation (4), we obtain

$$\boldsymbol{\alpha}_{ij}^{*(\boldsymbol{g})} = \frac{1}{s_0} \int\limits_{S_0} \boldsymbol{\beta}^P \times \boldsymbol{n} \exp (-2\pi i \boldsymbol{g\rho})\, dx_1 dx_2. \tag{15}$$

According to Kröner's theory (1958),

$$\eta_{ij} = \mathrm{Sym} (\epsilon_{ijk} \alpha_{ij,k}), \tag{16}$$

which is equation (5).

We define two tensors $\boldsymbol{A}(\boldsymbol{\rho})$ and $\boldsymbol{B}(\boldsymbol{\rho})$:

$$\boldsymbol{A}(\boldsymbol{\rho}) = \begin{pmatrix} 0 & 0 & \frac{1}{2}\left(\alpha_{11,2}^* - \alpha_{12,1}^*\right) \\ 0 & 0 & \frac{1}{2}\left(\alpha_{21,2}^* - \alpha_{22,1}^*\right) \\ \frac{1}{2}\left(\alpha_{11,2}^* - \alpha_{12,1}^*\right) & \frac{1}{2}\left(\alpha_{21,2}^* - \alpha_{22,1}^*\right) & 0 \end{pmatrix}, \tag{17}$$

and

$$\boldsymbol{B}(\boldsymbol{\rho}) = \begin{pmatrix} \alpha_{12}^* & \frac{1}{2}\left(\alpha_{22}^* - \alpha_{11}^*\right) & 0 \\ \frac{1}{2}\left(\alpha_{22}^* - \alpha_{11}^*\right) & -\alpha_{21}^* & 0 \\ 0 & 0 & 0 \end{pmatrix}. \tag{18}$$

Thus, for the plane distribution condition, the result is

$$\boldsymbol{\eta}(\boldsymbol{r}) = \boldsymbol{A}(\boldsymbol{\rho})\, \delta(x_3) + \boldsymbol{B}(\boldsymbol{\rho})\, \delta'(x_3). \tag{19}$$

Both $\boldsymbol{A}$ and $\boldsymbol{B}$ are periodic tensors, similar to α^*, which can also be expressed as Fourier series.

From Kröner's theory, the self-energy of one unit cell in periodic planar distribution dislocation is

$$E_s = \frac{1}{2s_0} \int\limits_{S_0} \eta_{ij}(x_1, x_2, x_3)\, \chi_{ij}(x_1, x_2, x_3)\, dx_1 dx_2 dx_3. \tag{20}$$

Here

$$\chi_{ij} = 2\mu \left(\chi'_{ij} + \frac{\nu}{1-\nu} \chi'_{kk} \delta_{ij}\right), \tag{21}$$

with shear moduli μ and Poisson ratio ν. Then, χ' is determined by

$$\nabla^4 \boldsymbol{\chi'} = \boldsymbol{\eta}. \tag{22}$$

Combining equations (17–19), and (22) yields the result

$$\nabla^4 \boldsymbol{\chi'} = \boldsymbol{A}\delta(x_3) + \left(\boldsymbol{B} - \boldsymbol{B}^{(0)}\right) \delta'(x_3) + \boldsymbol{B}^{(0)} \delta'(x_3). \tag{23}$$

Its solution, provided by Rey and Saada[13], is

$$\boldsymbol{\chi'} = \boldsymbol{A'} + \frac{1}{4} \boldsymbol{B}^{(0)} x_3^2\, \mathrm{sgn} x_3, \tag{24}$$

where

$$\boldsymbol{A'} = \sum_{\boldsymbol{g}}{}' \boldsymbol{A'}^{(\boldsymbol{g})}(x_3) \exp (2\pi i \boldsymbol{g\rho}) \exp (-2\pi g |x_3|), \tag{25}$$

$$\boldsymbol{A'}^{(\boldsymbol{g})}(x_3) = \left(\frac{1 + 2\pi g |x_3|}{32\pi^3 g^3}\right) \boldsymbol{A}^{(\boldsymbol{g})} - \frac{x_3 \boldsymbol{B}^{(\boldsymbol{g})}}{8\pi g}. \tag{26}$$

The tensors $\boldsymbol{\chi'}$, $\boldsymbol{\eta}$, and $\boldsymbol{\chi}$ are, therefore, formulated as above.

References

1. A. Sutton, R. Balluffi, *Interfaces in Crystalline Materials* (Oxford University Press, Oxford, 1996)
2. A. Trampert, F. Ernst, C.P. Flynn, H.F. Fischmeister, M. Ruhle, Acta Matall. Mater. **40**, S227 (1992)
3. G. Renaud, P. Guenard, A. Barbier, Phys. Rev. B **58**, 7310 (1998)
4. V.K. Lazarov, M. Weinert, S.A. Chambers, M. Gajdardziska-Josifovska, Phys. Rev. B **72**, 195401 (2005); J.M. Yang, J.J. Kim, K.S. Kim, W.G. Lee, M. Kawasaki, J. Electron Microscopy **55**, 1 (2006)
5. M.W. Finns, J. Phys.: Condens. Matter **8**, 5811 (1996)
6. T.P. Swiler, R.E. Loehman, Acta Mater. **48**, 4419 (2000); M. Christensen, S. Dudiy, G. Wahnström, Phys. Rev. B **65**, 045408 (2002); L.M. Liu, S.Q. Wang, H.Q. Ye, J. Phys.: Condens. Matter **16**, 5781 (2004)
7. R. Peierls, Proc. Phys. Soc. London **52**, 34 (1940); F. Nabarro, Proc. Phys. Soc. London **59**, 256 (1947)

8. J.H. Van der Merwe, Proc. Phys. Soc. London, Sect. A **63**, 616 (1950); J.H. Van der Merwe, J. Appl. Phys. **34**, 117 (1963)
9. Y. Yao, T. Wang, C. Wang, Phys. Rev. B **59**, 8232 (1999); Y. Yao, T. Wang, Acta Mater. **47** 3063 (1999)
10. N.I. Medvedeva, Y.N. Gornostyrev, O.Y. Kontsevoi, A.J. Freeman, Acta Mater. **52**, 675 (2004)
11. S.A.E. Johansson, M. Christensen, G. Wahnström, Phys. Rev. Lett. **95**, 226108 (2005)
12. J.P. Hirth, J. Lothe, *Theory of Dislocations*, 2nd edn. (Wiley, New York, 1982), p. 732
13. E. Kröner, *Theory of Crystal Defect* (summer school, Hrazany, 1964); C. Rey, G. Saada, Phil. Mag. **33**, 825 (1976)
14. V. Vitek, Cryst. Latt. Defects **5**, 1 (1974)
15. G. Schoeck, Phil. Mag. Lett. **77**, 141 (1998)
16. W. Bollmann, *Crystal Defects and Crystalline Interfaces*, (Springer, Berlin, 1970)
17. U. Schönberger, O.K. Anderson, M. Methfessel, Acta. Metall. Mater. **40**, S1 (1992)